

Boson-controlled quantum transport

A. Alvermann,¹ D. M. Edwards,² and H. Fehske¹

¹ *Institut für Physik, Ernst-Moritz-Arndt-Universität Greifswald, 17489 Greifswald, Germany*

² *Department of Mathematics, Imperial College London, London SW7 2AZ, United Kingdom*

We study the interplay of collective dynamics and damping in the presence of correlations and bosonic fluctuations within the framework of a newly proposed model, which captures the principal transport mechanisms that apply to a variety of physical systems. We establish close connections to the transport of lattice and spin polarons, or the dynamics of a particle coupled to a bath. We analyse the model by exactly calculating the optical conductivity, Drude weight, spectral functions, groundstate dispersion and particle-boson correlation functions for a 1D infinite system.

The motion of an electron or hole which interacts strongly with some background medium is a constantly recurring theme in condensed matter physics. Media which commonly occur are ordered spin backgrounds as in the t-J model of doped Mott insulators or vibrating lattices, as in the Holstein and quantized Su-Schrieffer-Heeger (SSH) models for polarons or charge density waves. A moving particle creates local distortions of substantial energy in the medium, e.g. local spin fluctuations, which may be able to relax. Their relaxation rate determines how fast the particle can move. In this sense particle motion is not free at all; the particle is continuously creating a string of distortions but can move on “freely” at a speed which gives the distortions time to decay. This picture is very general with wide applicability, e.g. to charge transport in high- T_c superconducting and colossal magnetoresistive materials, mesoscopic devices like quantum wires, and presumably even biological systems. [1]

In this Letter we investigate transport within some background medium by means of an effective lattice model with a novel form of electron-boson coupling. [2] The bosons correspond to local fluctuations of the background. To motivate the form of the model let us consider a hole in a 2D antiferromagnet. In a classical Neel background motion of the hole creates a string of misaligned spins. This ‘string effects’ strongly restricts propagation. [3] If however spins can exchange quantum-mechanically distortions of the spin background can ‘heal out’ by local spin fluctuations with a rate controlled by the exchange parameter J . This way the hole can move coherently with a bandwidth proportional to J . [4] Here we present a simpler spinless model which captures this two-fold physics within a generic framework.

Specifically, we consider the Hamiltonian

$$H = -t_f \sum_{\langle i,j \rangle} c_j^\dagger c_i - t_b \sum_{\langle i,j \rangle} c_j^\dagger c_i (b_i^\dagger + b_j) + \omega_0 \sum_i b_i^\dagger b_i \quad (1)$$

for fermionic particles (c_i^\dagger) coupled to bosonic fluctuations (b_i^\dagger) of energy ω_0 . H models two transport processes, one of unrestricted hopping $\propto t_f$, and a second of boson-controlled hopping $\propto t_b$. While for $t_b = 0$ the model reduces to that of a free particle, for $t_b \neq 0$ the

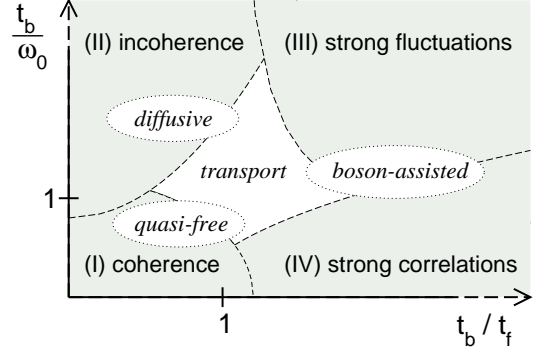


FIG. 1: Schematic view of the four physical regimes described by Hamiltonian (1), and the transport properties (see text).

physics of the model is governed by two ratios: The relative strength t_b/t_f of the two transport mechanisms, and the rate of bosonic fluctuations t_b/ω_0 . Therein the model also resembles common electron-phonon models like the Holstein or SSH model. Nevertheless it differs in that particle hopping creates a boson only on the site the particle leaves, and destroys a boson only on the site the particle enters. As a consequence the ‘string’ effect familiar from the t-J model is captured within the model, but also more complex features like in the 2D t-J model occur already in a 1D setting. In this contribution we study the model for a single particle in 1D at temperature $T = 0$.

We begin with a discussion of the physical regimes shown in Fig. 1. First, for small t_b/t_f (left side), transport takes place through unrestricted hopping. There, the model essentially describes motion of a particle coupled to a bosonic bath, when any bosonic fluctuations reduce the mobility of the particle. For small t_b/ω_0 (regime I), the number of bosons is small. The particle propagates almost coherently, and transport resembles that of a free particle. If t_b/ω_0 is larger (regime II), the number of bosons increases, and the bosonic timescale is slower than that of unrestricted hopping. Therefore bosonic fluctuations mainly act as random, incoherent scatterers, and the particle loses its coherence. The transport is then diffusive, with a short mean free path. In the second limiting case, for large t_b/t_f (right side), transport

takes mainly place through boson-controlled hopping, i.e. particle motion relies on the existence of bosons, which are created and consumed in the hopping process. For large t_b/ω_0 (regime III), transport is limited by strong scattering off uncorrelated bosonic fluctuations (similar to regime II). For small t_b/ω_0 however (regime IV), the bosons instantly follow the particle motion and strong correlations develop, leading to collective particle-boson dynamics. Note that boson-controlled hopping acts in two opposing ways: Depending on how many correlations between the bosons persist, it may either limit transport as a result of scattering off random fluctuations (regimes II and III), but may also enhance transport through correlated emission and absorption of bosons (regime IV).

For large t_b/t_f and small t_b/ω_0 , transport in the model resembles that of the hole-doped t-J-model. [4, 5] To make this connection more explicit, we perform the unitary transformation $b_i \mapsto b_i - t_f/2t_b$ of H :

$$H' = -t_b \sum_{\langle i,j \rangle} c_j^\dagger c_i (b_i^\dagger + b_j) - \lambda \sum_i (b_i^\dagger + b_i) + \omega_0 \sum_i b_i^\dagger b_i \quad (2)$$

(here a constant energy shift is dropped, which is proportional to the number of lattice sites N and guarantees finite results for $N \rightarrow \infty$). In (2) the coherent hopping channel is eliminated in favor of a boson relaxation term $\lambda \sum_i (b_i^\dagger + b_i)$. If $\lambda = \frac{\omega_0 t_f}{2t_b} > 0$, i. e. $t_f > 0$ in the original model, the decay of bosonic excitations allows for t - J -like quasiparticle (hole) transport. In the ‘classical’ limit $\lambda \rightarrow 0$ coherent quasiparticle motion is suppressed as in the t - J_z (Ising spin) model. Note that the limit $\omega_0 \rightarrow 0$ does not immediately lead to a semi-classical description established for the Holstein- and SSH-model since the electron does not couple exclusively to oscillator coordinates $\propto (b_i + b_i^\dagger)$.

For a quantitative analysis of transport in the different regimes we employ the optical conductivity $\text{Re } \sigma(\omega) = 2\pi D \delta(\omega) + \sigma_{\text{reg}}(\omega)$, where the regular part is

$$\sigma_{\text{reg}}(\omega) = \pi \sum_{n>0} \frac{|\langle n|j|0 \rangle|^2}{\omega_n} [\delta(\omega - \omega_n) + \delta(\omega + \omega_n)] . \quad (3)$$

Here $|n\rangle$ labels the eigenstates of the one-fermion system with excitation energy $\omega_n = E_n - E_0$, $|0\rangle$ is the ground-state. The current operator $j = j_f + j_b$ is given by

$$\begin{aligned} j_f &= it_f \sum_i c_{i+1}^\dagger c_i - c_i^\dagger c_{i+1} , \\ j_b &= it_b \sum_i c_{i+1}^\dagger c_i b_i^\dagger - c_i^\dagger c_{i+1} b_i - c_{i-1}^\dagger c_i b_i^\dagger + c_i^\dagger c_{i-1} b_i . \end{aligned} \quad (4)$$

The Drude weight D serves as a measure of the coherent, free particle like transport, and fulfils the f-sum rule

$$\int_{-\infty}^{\infty} \sigma(\omega) d\omega = 2\pi D + 2 \int_0^{\infty} \sigma_{\text{reg}}(\omega) d\omega = -\pi E_{\text{kin}} , \quad (5)$$

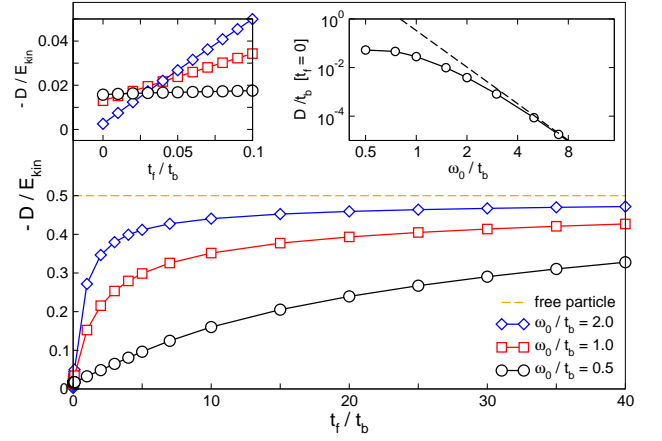


FIG. 2: (Color online) Drude weight D scaled to the kinetic energy E_{kin} . The left inset displays the region $t_f \gtrsim 0$ magnified, while the right inset shows D for $t_f = 0$ in dependence on ω_0 . The dashed curve gives the asymptotic result $D \simeq t_b^6/(3\omega_0^5) + O(t_b^8/\omega_0^7)$ for $\omega_0 \rightarrow \infty$.

where $E_{\text{kin}} = \langle 0|H - \omega_0 \sum_i b_i^\dagger b_i|0 \rangle$ is the kinetic energy. For a free particle ($t_b = 0$), the Drude weight is given by $D = t_f$, and the sum rule reads $-D/E_{\text{kin}} = 0.5$, while $-D/E_{\text{kin}} \ll 0.5$ for diffusive transport in the presence of strong fluctuations. We can therefore characterize the different transport regimes through the ratio $-D/E_{\text{kin}}$ (Fig. 2). The curve for $\omega_0/t_b = 2.0$ shows that in a wide range of t_f/t_b transport is quasi-free with $-D/E_{\text{kin}} \lesssim 0.5$. For smaller ω_0/t_b , as the number of fluctuations is larger, $-D/E_{\text{kin}}$ is decreased due to scattering. The smaller ω_0/t_b , the slower $-D/E_{\text{kin}}$ tends to its asymptotic values 0.5 for $t_f/t_b \rightarrow \infty$. This shows how the crossover from the coherent regime (I) with quasi-free transport to the incoherent regime (II) with diffusive transport is controlled by t_b/ω_0 . For small t_f/t_b , when boson-controlled hopping is the dominating transport process, D increases with decreasing ω_0 (left inset). This is the regime of boson-assisted transport, where transport is mediated by vacuum-restoring processes (see below). For the moment, we note, that D at $t_f = 0$ saturates with $\omega_0 \rightarrow 0$ (right inset), as one passes from the correlation dominated regime (IV) to the regime (III) of strong, uncorrelated fluctuations.

We complete our study by means of three quantities: First, the groundstate dispersion $E(k)$ provides the effective mass $1/m^* = \frac{\partial^2 E}{\partial k^2}|_{k=0}$, which is renormalized for $t_b \neq 0$. By Kohn’s formula, $D = 1/(2m^*)$. Second, we use the particle-boson correlation function

$$\chi_{ij} = \langle 0|b_i^\dagger b_i c_j^\dagger c_j|0 \rangle , \quad (6)$$

and third, the one-particle spectral function

$$A(k, \omega) = \sum_n |\langle n|c_k^\dagger|\text{vac} \rangle|^2 \delta(\omega - \omega_n) , \quad (7)$$

where $|\text{vac}\rangle$ denotes the particle vacuum. All quantities

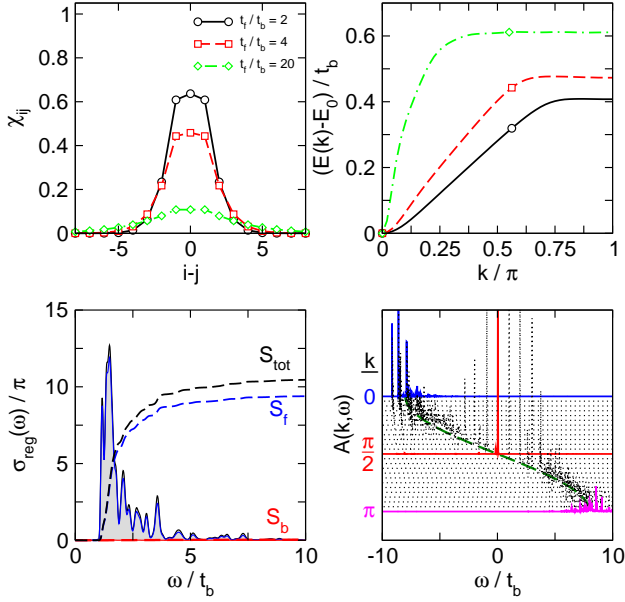


FIG. 3: (Color online) Top row: χ_{ij} (left) and $E(k) - E_0$ (right) for $\omega_0/t_b = 0.5$ and $t_f/t_b = 2, 4, 20$. Bottom row: $\sigma_{\text{reg}}(\omega)$ (left) for $t_f/t_b = 20$ and $A(k, \omega)$ (right) for $t_f/t_b = 4$. To analyze the relative importance of the two transport processes j_f and j_b , we show the corresponding contributions $\sigma_f(\omega)$, $\sigma_b(\omega)$ to $\sigma_{\text{reg}}(\omega)$ separately (note that generally $\sigma_{\text{reg}}(\omega) \neq \sigma_f(\omega) + \sigma_b(\omega)$). S_{tot} (and similar S_f , S_b) denotes the integrated conductivity $S_{\text{tot}}(\omega) = \int_0^\omega \sigma_{\text{reg}}(\omega') d\omega'$.

have been calculated with exact numerical techniques (Lanczos diagonalization and kernel polynomial methods [6]). We employed a basis construction for the many-particle Hilbert space that is variational for an infinite lattice. [7] This guarantees data of extremely high precision, free of finite size effects.

Let us first discuss the ‘incoherent’ or ‘diffusive’ regime (II) (see Fig. 3). As expected, the regular part of the optical conductivity is dominated by a broad incoherent absorption continuum, and $-D/E_{\text{kin}}$ is small. This resembles the situation for a large Holstein (lattice) polaron, where the role of bosonic fluctuations is taken by optical phonons. [8] χ_{ij} shows that bosonic fluctuations are rather weakly correlated. Of course, they form a cloud surrounding the particle, but are not further correlated. The spectral function $A(k, \omega)$ supports this picture. The spectral weight is distributed along the ‘free’ dispersion $-2t_f \cos k$, like for a weakly bound particle-boson excitation. Around $k = 0$ and $k = \pm\pi$, the overdamped character of particle motion is very prominent. Comparing with $E(k)$, we see that the quasi-particle weight is negligible away from $k = 0$, and a well-defined quasi-particle band does not exist. Somewhat surprisingly, for $k = \pm\pi/2$ almost all weight resides in a single coherent peak at $\omega = 0$. A particle injected with $k = \pm\pi/2$ therefore propagates almost unaffected by bosonic fluctuations. In a sense, the system is transparent at this

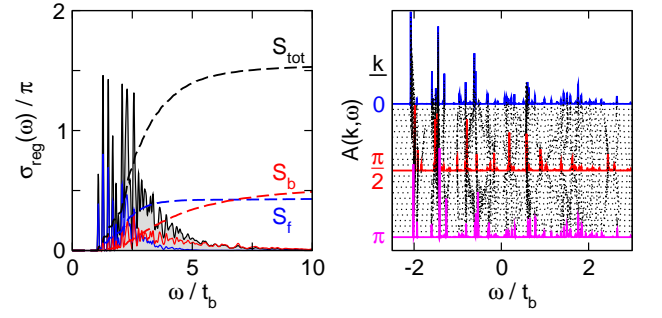


FIG. 4: (Color online) $\sigma_{\text{reg}}(\omega)$ for $\omega_0/t_b = 1.0$, $t_f/t_b = 2.0$ (left), and $A(k, \omega)$ for $\omega_0/t_b = 0.5$, $t_f/t_b = 0.04$ (right).

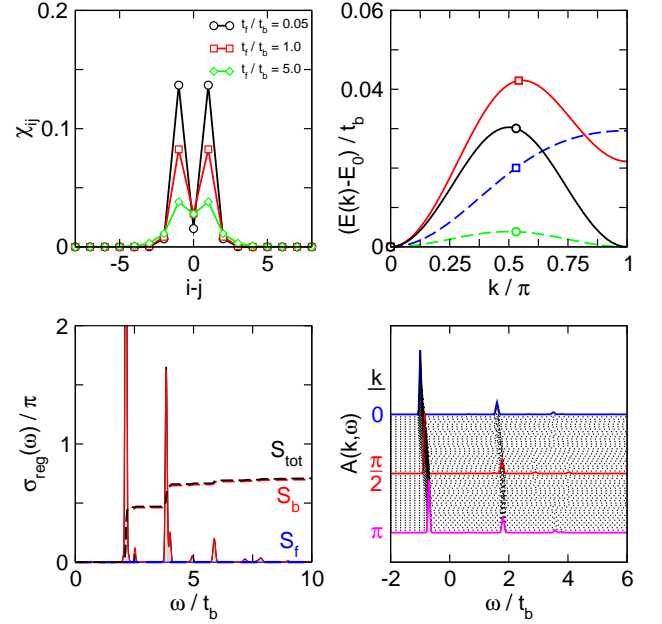


FIG. 5: (Color online) Top left: χ_{ij} for $\omega_0/t_b = 2$ and $t_f/t_b = 0.05$ (circles), 1.0 (squares), 5.0 (diamond). Top right: $E(k) - E_0$ for $\omega_0/t_b = 1$ (solid) and $\omega_0/t_b = 2$ (dashed), with $t_f/t_b = 0$ (circles), $t_f/t_b = 0.01$ (squares). Bottom row: $\sigma_{\text{reg}}(\omega)$ (left) and $A(k, \omega)$ (right) for $\omega_0/t_b = 2$, $t_f/t_b = 0.1$.

energy, similar to e.g. a double well at certain resonant energies.

From the diffusive regime, we can evolve in two directions. First, if we increase t_b/t_f (\rightsquigarrow regime (III)), the contribution of boson-controlled hopping to the conductivity begins to dominate (see Fig. 4, left panel). Still, transport is mainly diffusive (cf. Fig. 2). If we further increase t_b/t_f while keeping t_b/ω_0 large (inside regime (III)), strong but uncorrelated bosonic fluctuations develop. As a result, the spectral function $A(k, \omega)$ becomes fully incoherent (right panel), and $-D/E_{\text{kin}}$ is small. Apparently, the large number of bosonic fluctuations prevents strong correlations (cf. χ_{ij} in Fig. 3). In the second direction, for large t_b/t_f and small t_b/ω_0 (regime (IV)), the number of fluctuations is reduced. Then, strong cor-

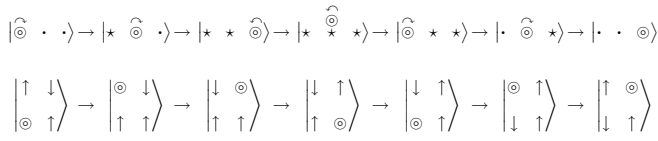


FIG. 6: Lowest order vacuum-restoring process (upper row), which is a one-dimensional representation of the ‘Trugman path’ [5] in a Néel-ordered spin background (lower row). In steps 1–3, three bosons are excited, which are consumed in steps 4–6. Note how the correlated many-particle vacuum of the spin model is translated to the bosonic vacuum.

relations evolve (see χ_{ij} in Fig. 5). The conductivity is now entirely given by the contribution from boson-controlled hopping, but does not show the absorption continuum we found for diffusive transport (note that, although $-D/E_{\text{kin}}$ must be small for large t_b/t_f , it is much larger than for larger t_b/ω_0). Instead, both $\sigma_{\text{reg}}(\omega)$ and $A(k, \omega)$ consist of a few, well separated peaks. This indicates, that here the model shows collective particle-boson dynamics, i. e. a well-defined quasi-particle exists, like a spin/magnetic polaron in the t-J-model. [4, 9] As a particular feature of the correlated transport mechanism which dominates for $t_b/t_f \gg 1$, the quasi-particle dispersion $E(k)$ develops a $k \rightarrow k + \pi$ symmetry for $t_b/t_f \rightarrow \infty$. At $t_f = 0$ the model therefore shows an electronic topological transition, for which the hole doped t-J-model provides a specific example.

The correlated transport mechanism for $t_b/t_f \gg 1$ is best understood in the limit $t_f = 0$. Then, the particle can only move by creating bosonic fluctuations, i.e. transport is fully boson-assisted. Moving by L sites costs energy $L\omega_0$, which is just the string effect and tends to localize the particle. However, there exist processes that propagate the particle but restore the boson vacuum in their course. The lowest order process of this kind comprises 6 steps, promoting the particle by 2 sites (Fig. 6). By this and similar higher order processes the particle is itinerant even at $t_f = 0$, with a finite, though small, Drude weight. Since in any hop the boson number changes by one, any vacuum-restoring process propagates the particle by an even number of sites. This immediately explains, why $E(k)$ for $t_f = 0$ has period π . The weight of the lowest order process shown in Fig. 6 scales as t_b^6/ω_0^5 (cf. Fig. 2). Accordingly, boson-assisted transport dominates for large $(t_b/\omega_0)^5(t_b/t_f)$. In this regime, the mobility of the particle increases if ω_0 decreases, as vacuum-restoring processes become energetically more favorable. This explains the opposite dependence of D on ω_0 for $t_f/t_b \ll 1$ and $t_f/t_b \gtrsim 1$. In the plot of the Drude weight the transition from uncorrelated, diffusive to correlated, boson-assisted transport therefore leads to a crossing of the curves at about $t_f/t_b \sim 0.05$ (see Fig. 2, left inset). This substantiates our initial

remark that bosonic fluctuations act in two competing ways: While they limit transport by unrestricted hopping if strong but weakly correlated, they assist transport by boson-controlled hopping in the regime of strong correlations. Equally important, the same boson-assisted mechanism which allows for transport is limited by itself, because strong correlations cannot persist in the presence of many fluctuations: The Drude weight $D_{t_f=0}$ for $t_f = 0$ increases with decreasing ω_0 as we discussed, but finally saturates. The large number of bosonic fluctuations, which become increasingly uncorrelated for small ω_0 , interfere with the correlated boson excitations in the vacuum-restoring transport processes, restricting their efficiency. Note that these fundamental physical mechanisms are not enforced in the model, but emerge naturally from the competition between uncorrelated scattering and correlation-induced transport.

To conclude, the model that we propose provides a reduced but realistic description of fundamental aspects of transport in the presence of bosonic fluctuations. Topics of current interest become accessible within the comprehensive framework established. Despite its seemingly simple form, the model covers very different physical regimes, identified e.g. by the Drude weight. For these regimes, we establish links to important many-body systems like lattice or spin polarons, and could thereby demonstrate the relevance of the model. Based on these results, the model will certainly prove useful for further studies, e.g. on the possibility of pairing for two particles, or on topological phase transitions for finite densities. The whole phase diagram for finite density and temperature is open for investigation.

We acknowledge helpful discussions with G. Wellein and financial support by DFG through SFB 652.

-
- [1] D. M. Newns and C. C. Tsuei, cond-mat/0606223 (2006); L. G. L. Wegener and P. B. Littlewood, Phys. Rev. B **66**, 224402 (2002); S. Komineas, G. Kalosakas, and A. R. Bishop, Phys. Rev. E **65**, 061905 (2002).
 - [2] D. M. Edwards, Physica B **378-380**, 133 (2006).
 - [3] W. F. Brinkman and T. M. Rice, Phys. Rev. B **2**, 1324 (1970).
 - [4] C. L. Kane, P. A. Lee, and N. Read, Phys. Rev. B **39**, 6880 (1989).
 - [5] S. A. Trugman, Phys. Rev. B **37**, 1597 (1988).
 - [6] A. Weiße, G. Wellein, A. Alvermann, and H. Fehske, Rev. Mod. Phys. **78**, 275 (2006).
 - [7] J. Bonča, S. A. Trugman, and I. Batistić, Phys. Rev. B **60**, 1633 (1999).
 - [8] B. Bäuml, G. Wellein, and H. Fehske, Phys. Rev. B **58**, 3663 (1998).
 - [9] J. R. Schrieffer, X.-G. Wen, and S.-C. Zhang, Phys. Rev. Lett. **60**, 944 (1988).